

Angiographic Evaluation of Feeding Arteries of Hepatocellular Carcinoma in the Caudate Lobe of the Liver

Shiro Miyayama · Masashi Yamashiro ·
Yuki Hattori · Nobuaki Orito · Ken Matsui ·
Kazunobu Tsuji · Miki Yoshida · Osamu Matsui

Received: 12 July 2010 / Accepted: 24 October 2010

© Springer Science+Business Media, LLC and the Cardiovascular and Interventional Radiological Society of Europe (CIRSE) 2010

Abstract

Purpose To evaluate the origins of feeders of hepatocellular carcinoma (HCC) in the caudate lobe (S1).

Materials and Methods Eighty-eight HCCs (mean diameter 21.4 mm) were treated by chemoembolization. The tumor-feeding caudate artery was confirmed when a tumor stain was demonstrated on angiogram and iodized oil was accumulated into the HCC and S1 on computed tomography (CT). The origins were divided into R₁ (right proximal), R₂ (right distal), L₁ (left proximal), L₂ (left distal), A (anterior segmental), P (posterior segmental), M (middle hepatic or medial segmental), Ph (proper hepatic), Ch (common hepatic), and Ex (extrahepatic). The origins of feeders supplying HCCs in the Spiegel lobe (SP; n = 36), the paracaval portion (PC; n = 38), and the caudate process (CP; n = 14) were also analyzed.

Results One hundred sixteen feeders were identified: 11 (9.5%) arose from R₁; 21 (18.1%) arose from R₂; nine arose (0.9%) from L₁; 15 (12.9%) arose from L₂; 24 (20.7%) arose from A; 25 (21.6%) arose from P; seven (6.0%) arose from M; one (0.9%) arose from Ph; and three (2.6%) arose from Ex. HCCs in the SP and the PC were fed by feeders from both hepatic arteries (the ratios of right to left were 3:2 and 3:1, respectively), and HCCs in the CP were dominantly fed by feeders from the right hepatic artery.

Conclusion The caudate artery most frequently arises from the right hepatic artery, followed with almost equal frequency by the left hepatic, the anterior segmental, and the posterior segmental artery. The origins of the caudate arteries differ according to the subsegmental locations.

Keywords Hepatocellular carcinoma · Caudate lobe · Feeding artery · Transcatheter arterial chemoembolization

Introduction

The caudate lobe is centrally located in the liver between the right and left lobes of the liver and near the hepatic hilus and the inferior vena cava. Because of this anatomic location, hepatocellular carcinoma (HCC) arising in the caudate lobe is difficult to treat [1]. Surgical resection of the caudate lobe has a high mortality rate because of large amounts blood loss, a high rate of postoperative complications, and a high tumor-recurrence rate [2, 3]. Percutaneous ablation therapy, such as ethanol injection and radiofrequency ablation, is a useful alternative treatment [4–6]; however, the procedure might be technically difficult because of the deep tumor location and adjacent large vessels. Therefore, transcatheter arterial chemoembolization (TACE) plays an important role in the treatment of HCC in the caudate lobe, although local tumor recurrence is frequently observed after TACE [4, 7, 8].

Because there are usually multiple caudate arteries arising from the right, left, and middle hepatic arteries, as well as from the extrahepatic collateral vessels, 16–31% of HCCs in the caudate lobe are fed by multiple branches arising from different origins [7–12]. These factors might make it more difficult to control HCC in the caudate lobe using TACE [7, 8, 10]. Recognition of vascular anatomy

S. Miyayama (✉) · M. Yamashiro · Y. Hattori · N. Orito ·
K. Matsui · K. Tsuji · M. Yoshida
Department of Diagnostic Radiology, Fukuiken Saiseikai
Hospital, Fukui, Japan
e-mail: s-miyayama@fukui.saiseikai.or.jp

O. Matsui
Department of Radiology, Kanazawa University Graduate
School of Medical Science, Kanazawa, Japan

supplying HCCs in the caudate lobe is key to performing effective TACE. Thus, the purpose of our study was to retrospectively analyze the origins of the HCC-feeding arteries in the caudate lobe and to evaluate the anatomic variations of tumor-feeding arteries in relation to subsegments of the caudate lobe.

Materials and Methods

We performed a retrospective study to evaluate the origins of tumor-feeding caudate arteries. This was a retrospective study using imaging data and clinical records with no change in patient care; Institutional Review Board approval is not required at our institution for this type of study. Written informed consent was obtained from each patient before the TACE procedure.

Patients

Between February 2002 and February 2010, 88 HCCs originating in the caudate lobe were detected in 84 patients. There were 48 men and 36 women, and the mean patient age was (mean \pm SD) 70.2 \pm 7.3 years (range 45–86). All patients had liver cirrhosis. This was related to hepatitis C in 71 patients, to hepatitis B in four patients, and to alcohol in three patients. The etiology was unknown in six patients. The diagnosis of HCC was established by imaging findings: (1) characteristic nodular enhancement on the arterial phase and wash out on the delayed phase images on computed tomography (CT) and/or magnetic resonance imaging; (2) nodular stain on angiography and/or CT during hepatic arteriography obtained using conventional CT or cone-beam CT; and (3) nodular perfusion defect on CT during arterial portography obtained using conventional CT or cone-beam CT. Histological confirmation was not obtained in any patient in this series. Mean tumor diameter was 21.4 \pm 11.0 mm (range 8–62). Fifty-two patients (61.9%) had a history of TACE for HCC before detection of HCC in the caudate lobe. Thirty-two patients (38.1%) had no treatment history for HCC.

Hepatic Angiography and the TACE Procedure

Arteriograms of the celiac and superior mesenteric arteries were routinely performed using a 4F catheter. Common hepatic or proper hepatic arteriogram was also performed in all patients using a 4F catheter or a 1.8F-tip (Carnelian Pixie; Tokai Medical Products, Kasugai, Japan), a 2F-tip (Progreat α ; Terumo, Tokyo, Japan), or a 2.4F-tip (Microferret; Cook, Bloomington, IN, USA) microcatheter. Arteriograms of extrahepatic vessels, such as the right inferior phrenic artery, the right renal capsular artery, and

the left gastric artery, were obtained when the tumor stain was unclear on hepatic arteriography.

All TACE procedures were performed through the caudate arteries were selectively performed using a microcatheter. The microcatheter with its tip bent into a J shape by steam was used for all procedures to facilitate insertion into small caudate arteries that branched at acute angles. To navigate the microcatheter, a 0.016-inch guidewire (GT-wire; Terumo) was used. When selection of the feeding branch by the 0.016-inch guidewire was difficult, a 0.012-inch guidewire (GT-wire; Terumo) was used. After the microcatheter was inserted into the target branch, 0.5 ml 2% lidocaine (Xylocaine; Fujisawa, Osaka, Japan) was intra-arterially injected to prevent pain and vasospasm. First, a mixture of 2–4 ml iodized oil (Lipiodol; Andre Guerbet, Aulnay-sous-Bois, France) and anticancer drugs (10–20 mg epirubicin [Farmorbicin; Kyowa Hakko, Tokyo, Japan] and 2–4 mg mitomycin C [Mitomycin; Kyowa Hakko]) was injected and this was followed by injection of gelatin sponge particles. The total amount of iodized oil injected in a single procedure was determined based on the tumor size (volume almost equal to the diameter of the tumor, e.g., a 3-cm tumor received 3 ml iodized oil). Until December 2006, gelatin sponge (Gelfoam; Upjohn, Kalamazoo, MI, USA) particles that were cut into approximately 1-mm cubes were used. Since January 2007, commercially available gelatin sponge particles (Gelpart; Nippon Kayaku, Tokyo, Japan) 1 mm in diameter have been used. TACE through extrahepatic collateral vessels was also performed when the blood supply to the tumor was demonstrated. Unenhanced CT was obtained 1 week after TACE in all patients to check for iodized oil accumulation in HCCs in the caudate lobe.

Definition of the Origin of the Caudate Artery

We defined the embolized branch as the tumor-feeding caudate artery when a tumor stain was demonstrated on arteriogram and iodized oil showed accumulation in the HCC and the caudate lobe on CT obtained 1 week after TACE. If CT 1 week after TACE showed a tumor portion in which iodized oil was not accumulated, an additional TACE was performed 2–6 months later according to the residual tumor size and patient's medical condition. When the residual tumor was supplied by another caudate artery that had initially not been embolized, the caudate artery was also defined as the tumor-feeding caudate artery.

The origins of the caudate arteries were divided into R₁, R₂, L₁, L₂, A, P, M, Ph, Ch, and Ex (Fig. 1). The caudate lobe was divided into three subsegments according to the classification proposed by Kumon [13] (Fig. 2): the Spiegel lobe (SP), the paracaval portion (PC), and the caudate process (CP). The origins of the caudate arteries supplying

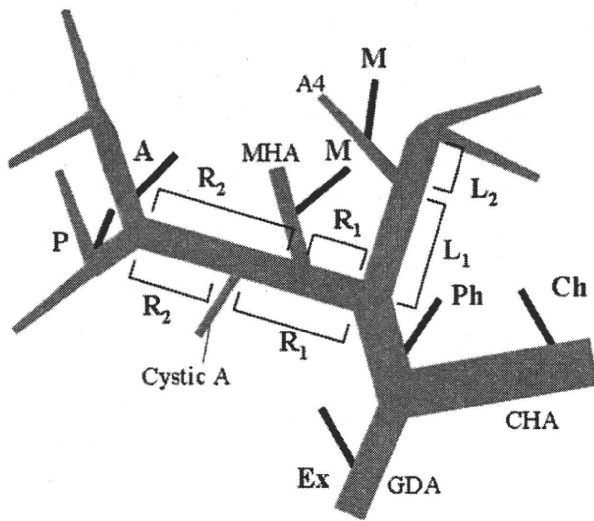


Fig. 1 The definition of the origins of tumor-feeding caudate arteries. *R₁* (right proximal) arising from the right hepatic artery (RHA) between its origin and the middle hepatic artery (MHA) bifurcation or the cystic artery bifurcation if the MHA was not present; *R₂* (right distal) arising from the RHA between the MHA (or cystic artery) bifurcation and the bifurcation of the anterior and posterior segmental artery of the RHA. If both the MHA and the cystic artery were not present, the RHA was divided into the two equal parts; *L₁* (left proximal) arising from the left hepatic artery (LHA) between its origin and the medial segmental artery (A4) bifurcation; *L₂* (left distal) arising from the LHA between the A4 bifurcation and the umbilical portion of the LHA. If the A4 did not arise from the LHA, the LHA was divided into the two equal parts; *A* arising from the anterior segmental artery of the right hepatic artery; *P* arising from the posterior segmental artery of the right hepatic artery; *M* arising from the MHA or the A4; *Ph* arising from the proper hepatic artery; *Ch* arising from the common hepatic artery; and *Ex* arising from the extrahepatic vessels

the HCCs in each subsegment were also analyzed. When a tumor was located between two subsegments, the tumor was classified based on the one subsegment in which it was dominantly located.

Results

Origins of the Tumor-Feeding Caudate Arteries

Eighty-two tumors in the caudate lobe of 78 patients were treated by a single TACE session. The remaining six tumors in six patients were treated with two TACE sessions because of incomplete iodized oil accumulation in the entire tumor on CT obtained after the initial TACE session. In total, 116 caudate arteries were identified, and all were selectively embolized during TACE, including six

additional TACE sessions (Table 1). During TACE, 1.3 ± 0.5 feeding arteries (range 1–3) were embolized/tumor. Eleven caudate arteries (9.5%) were derived from *R₁*; 21 (18.1%) from *R₂*; nine (7.8%) from *L₁*; 15 (12.9%) from *L₂*; 24 (20.7%) from *A*; 25 (21.6%) from *P*; seven (6.0%) from *M*; one (0.9%) from *Ph*; and three (2.6%) from *Ex*. No caudate arteries were derived from *Ch* in the present series. Eighty-one caudate arteries (70.4%) were derived from the right hepatic arterial system (*R₁* + *R₂* + *A* + *P*), and 31 (27.0%) were derived from the left hepatic arterial system (*L₁* + *L₂* + *M*). In total, 27.6% of the caudate arteries were derived from the right hepatic artery (*R₁* + *R₂*), 20.7% from the left hepatic artery (*L₁* + *L₂*), 20.7% from the anterior segmental artery of the right hepatic artery, 21.6% from the posterior segmental artery of the right hepatic artery, and 6.0% from the middle hepatic artery or the medial segmental artery.

Origins of the Caudate Arteries Supplying HCCs in the SP

Our findings are listed in Table 2. There were 36 tumors with a mean diameter of 22.3 ± 11.9 mm (range 8–62 mm) in the SP. Twenty-five tumors (69.4%) were supplied by a single tumor-feeding caudate artery. Among these, 15 tumors were supplied by the feeding artery derived from the right hepatic arterial system (*R₁* [*n* = 2], *R₂* [*n* = 7], *A* [*n* = 2], *P* [*n* = 4]) (Fig. 3), and nine were supplied by the feeding artery derived from the left hepatic arterial system (*L₁* [*n* = 3], *L₂* [*n* = 4], *M* [*n* = 2]). The remaining tumor was supplied by a feeding artery derived from the right inferior phrenic artery (*Ex*). Eleven tumors (30.6%) had two feeding arteries. Among these, eight were supplied by feeding arteries derived from the right (*R₁* [*n* = 2], *R₂* [*n* = 1], *A* [*n* = 4], *P* [*n* = 1]) and the left hepatic arterial system (*L₁* [*n* = 3], *L₂* [*n* = 4], *M* [*n* = 1]), respectively (Figs. 4 and 5). One tumor was supplied by two feeding arteries derived from *A*. The remaining two tumors were supplied by feeding arteries derived from the left hepatic arterial system (*L₂* [*n* = 1], *M* [*n* = 1]) and *Ex* (the right inferior phrenic artery [*n* = 1]) as well as the accessory left gastric artery [*n* = 1]), respectively. In total, there were 47 tumor-feeding caudate arteries. Twenty-five tumor-feeding arteries arose from the right hepatic arterial system, 19 from the left hepatic arterial system, and three from the extrahepatic collaterals. The diameters of three tumors that were supplied by extrahepatic collaterals were 17, 26, and 48 mm, respectively. All three tumors were detected in patients with no histories of TACE, including one patient who had undergone hepatic resection. All three tumors were located at the anterior (*n* = 1) or posterior (*n* = 2) surface of the SP.

Fig. 2 Schematic presentation of subsegments of the caudate lobe

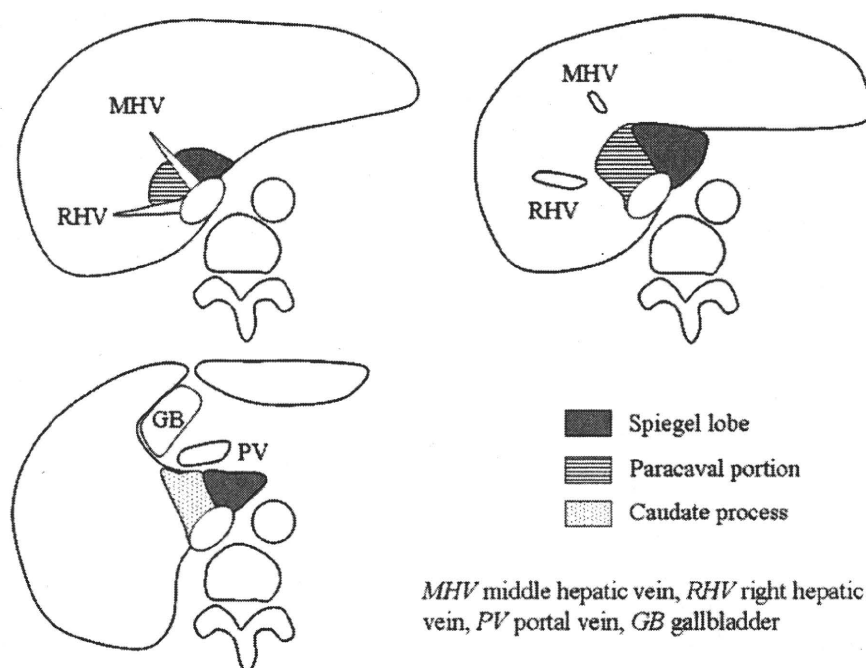


Table 1 Origins of tumor-feeding arteries of 88 HCCs in the caudate lobe

Origin	No. (%)	
R ₁	11 (9.5)	32 (27.6%)
R ₂	21 (18.1)	
L ₁	9 (7.8)	24 (20.7%)
L ₂	15 (12.9)	
A	24 (20.7)	
P	25 (21.6)	
M	7 (6.0)	
Ph	1 (0.9)	
Ch	0 (0)	
Ex	3 (2.6)	
Total	116 (1.3 ± 0.5 arteries/tumor)	

Mean tumor diameter 21.4 ± 11.0 mm [range 8–62]

Origins of the Caudate Arteries Supplying HCCs in the PC

Our findings are listed in Table 3. There were 38 tumors with a mean diameter of 20.2 ± 9.3 mm (range 8–47) in the PC. Twenty-nine tumors (76.3%) were supplied by a single feeding artery. Among these, 20 tumors were supplied by the caudate artery derived from the right hepatic arterial system (R₁ [n = 4], R₂ [n = 7], A [n = 3], P [n = 6]). Nine were supplied by the caudate artery derived from the left hepatic arterial system (L₁ [n = 1], L₂ [n = 5], M [n = 3]). Seven tumors (18.4%) had two feeding arteries. Among these, three tumors were supplied by feeding arteries derived from the right (A [n = 1], P

Table 2 Feeding arteries of 36 HCCs in the SP

No. of feeders	No. of tumors (%)	Site	Origin	Tumor		
1	25 (69.4)	R	R ₁	2		
			R ₂	7		
			A	2		
			P	4		
			L	L ₁	3	
				L ₂	4	
		Ex	M	2		
			Ex ^a	1		
		2	11 (30.6)	R + L	R ₁ , L ₁	1
					R ₁ , L ₂	1
					R ₂ , L ₁	1
					A, L ₁	1
					A, L ₂	2
A, M	1					
P, L ₂	1					
R × 2	A × 2	1				
	L ₂ , Ex ^b	1				
M, Ex ^a	1	M, Ex ^a	1			

Mean tumor diameter 22.3 ± 11.9 mm [range 8–62]. The ratio of R:L = 25:19

^a Arising from the right inferior phrenic artery

^b Arising from the accessory left gastric artery

[n = 2]) and the left hepatic arterial system (L₁ [n = 2], L₂ [n = 1]), respectively. Four tumors were supplied by two feeding arteries derived from the right hepatic arterial system (R₂ and P [n = 1], A × 2 [n = 1], A and P

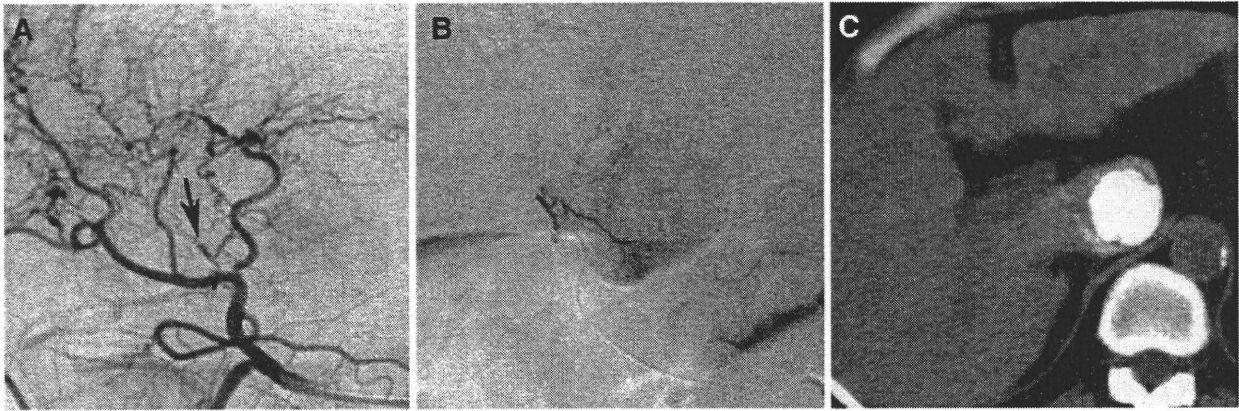


Fig. 3 A 45-year-old woman with HCC in the SP. **A** Common hepatic arteriogram showed that the caudate artery derived from the right hepatic artery proximal to the middle hepatic artery (*arrow*).

B The caudate artery was selected, and TACE was performed. **C** CT obtained 1 week after TACE showed dense iodized oil accumulation in HCC in the SP

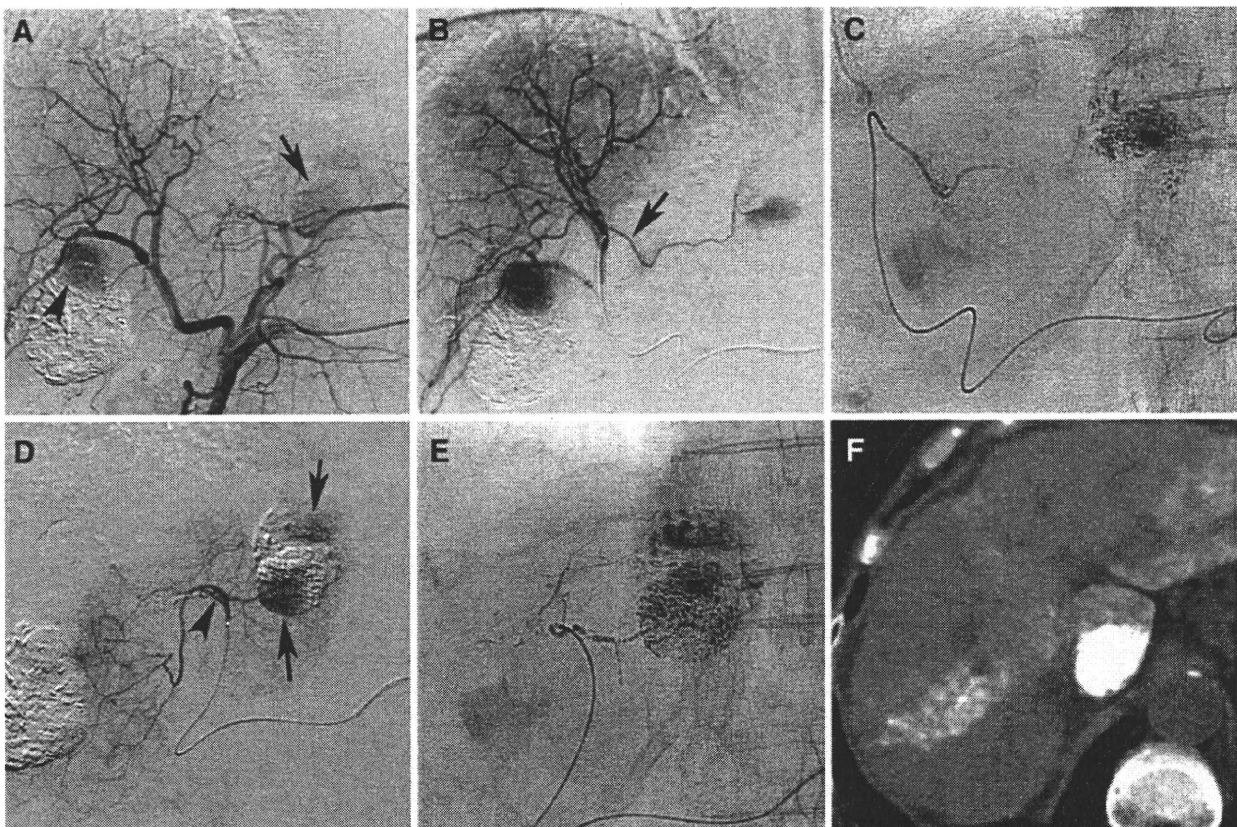


Fig. 4 A 73-year-old woman with HCC in the SP. **A** Common hepatic arteriogram showed tumor stains in the caudate lobe (*arrow*) and in the right lobe near the previously embolized tumor (*arrowhead*). **B** Arteriogram of the anterior segmental artery of the right hepatic artery showed tumor stains. The arrow shows the caudate artery. **C** The caudate artery was selected, and TACE was performed.

Subsequently, the tumor in the right lobe was also embolized (not shown). **D** Arteriogram of the medial segmental artery showed a residual tumor stain of HCC in the caudate lobe (*arrows*). The *arrowhead* shows the caudate artery. **E** The caudate artery was selected, and TACE was performed. **F** CT obtained 1 week after TACE showed dense iodized oil accumulation in HCC in the SP

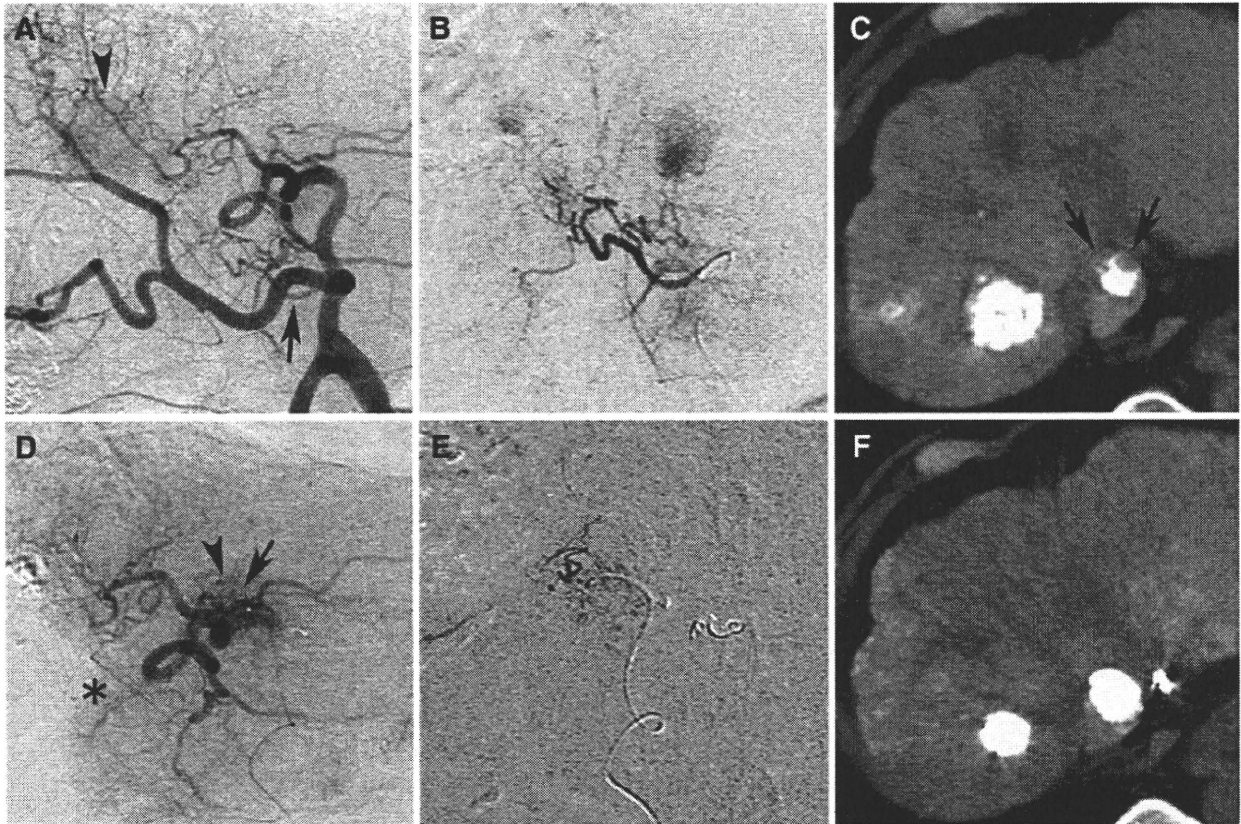


Fig. 5 A 78-year-old man with HCC in the SP. **A** Common hepatic arteriogram showed that the caudate artery derived from the proximal right hepatic artery (*arrow*). Another tumor stain in the right lobe of the liver was also seen (*arrowhead*). **B** Selective arteriogram of the caudate artery showed two tumor stains. This vessel was embolized. Subsequently, the tumor in the right lobe was also embolized (not shown). **C** CT obtained 1 week after TACE showed that iodized oil was densely accumulated in the tumor in the SP, but a tumor portion without iodized oil accumulation was seen (*arrows*). Iodized oil was

also densely accumulated other tumors in the right lobe of the liver. **D** Arteriogram of the left hepatic artery obtained 4 months after initial TACE showed that the caudate artery derived from the distal left hepatic artery (*arrow*), and a residual tumor stain (*arrowhead*) was seen. The falciform artery was also seen (*asterisk*). **E** The caudate artery was selected and embolized. **F** CT obtained 1 week after second TACE showed dense iodized oil accumulation in the entire tumor

[$n = 2$]). The remaining two tumors (5.3%), which were 14 and 23 mm in diameter, respectively, were supplied by three feeding arteries derived from the right hepatic arterial system at R_1 , A, and P and R_2 , A, and P, respectively (Fig. 6). In total, there were 49 tumor-feeding caudate arteries. Thirty-seven tumor-feeding caudate arteries arose from the right hepatic arterial system, and 12 arose from the left hepatic arterial system.

Origins of the Caudate Arteries Supplying HCCs in the CP

Our findings are listed in Table 4. There were 14 tumors with a mean diameter of 21.8 ± 12.9 mm (range 12–49) in the CP. Nine tumors (64.3%) were supplied by a single feeding artery. Among these, seven tumors were supplied by a feeding artery derived from the right hepatic arterial system (R_1 [$n = 1$], A [$n = 3$], P [$n = 3$]) (Fig. 7); one

was supplied by the caudate artery derived from M; and one was supplied by the caudate artery derived from Ph. Four tumors were supplied by two feeding arteries derived from the right hepatic arterial system (R_1 and R_2 [$n = 1$], R_2 and A [$n = 1$], A \times 2 [$n = 1$], P \times 2 [$n = 1$]). The remaining tumor (7.1%), which was 13 mm in diameter, was supplied by three feeding arteries derived from the right hepatic arterial system at R_2 , P, and P, respectively. In total, there were 20 tumor-feeding caudate arteries. Eighteen tumor-feeding arteries arose from the right hepatic arterial system; one arose from the middle hepatic artery; and one arose from the proper hepatic artery.

Discussion

A cadaver dissection study by Mizumoto et al. [10] reported that the caudate arteries arose from the posterior

Table 3 Feeding arteries of 38 HCCs in the PC

No. of feeders	No. of tumors	Site	Origin	Tumor
1	29 (76.3%)	R	R ₁	4
			R ₂	7
			A	3
		L	P	6
			L ₁	1
			L ₂	5
			M	3
2	7 (18.4%)	R + L	A, L ₁	1
			P, L ₁	1
			P, L ₂	1
		R × 2	R ₂ , P	1
		A × 2	1	
A, P	2			
3	2 (5.3%)	R × 3	R ₁ , A, P	1
			R ₂ , A, P	1

Mean tumor diameter 20.2 ± 9.3 mm [range 8–47]. The ratio of R:L = 37:12

segmental artery of the right hepatic artery and the left hepatic artery in 32.1% of 106 cadavers; from the posterior segmental artery of the right hepatic artery and the middle hepatic artery in 26.4% of cadavers; and from these three arteries in 20.8% of cadavers. In another cadaver study by Suzuki [11], the right-side caudate artery arose from the posterior segmental artery of the right hepatic artery in 89.7% of cadavers, and only 9.3% arose from the right hepatic artery. However, in previous angiographic observations, the most common origin of the caudate artery was the right hepatic artery [7–9]. In addition, the incidences of the caudate artery derived from the left hepatic artery and the posterior segmental artery of the right hepatic artery were low compared with those reported in dissection studies [7]. The cause of this discrepancy between dissection study and angiographic study is speculated as follows: First, the caudate artery derived from the right hepatic artery can easily be identified on arteriogram because there is less superimposition of the hepatic branches. Second, because the left hepatic lobe has a limited depth, identification of the caudate artery is difficult even on stereo angiogram [7]. Finally, the caudate artery derived from the posterior segmental artery is frequently difficult to recognize as the caudate artery on arteriogram because it mimics the branches of the posterior segmental artery of the right hepatic artery [7]. Therefore, there is a significant limitation in nonselective angiographic evaluations of the caudate arteries. Moreover, some small caudate branches derived from the proximal portion of the hepatic artery might be killed during preparation in dissection studies.

With advances in catheter technology, superselective catheterization and chemoembolization at the most distal level of the subsegmental artery of the liver have become possible [14, 15], even through the caudate arteries [9, 12, 16]. Iodized oil injected during the TACE procedure can clearly indicate the vascular territory of the embolized branch on CT. In the present study, we could easily recognize that the embolized branch was the caudate artery when iodized oil was retained in the caudate lobe, including the tumor, on CT obtained 1 week after TACE. This evaluation method facilitates precise identification of the caudate artery, although this artery frequently mimics other hepatic branches on arteriogram alone.

In the present study, the most frequent origin of the tumor-feeding caudate artery was the right hepatic artery, followed with almost equal frequency by the left hepatic artery, the anterior segmental artery, and the posterior segmental artery of the right hepatic artery. Our results suggest that the caudate artery actually can be identified from the right hepatic artery most frequently and not just because it can easily be identified on arteriogram due to less superimposition of the hepatic branches. Among the caudate arteries derived from the right and left hepatic arteries, it dominantly arose from the distal portion (R₂ and L₂). In addition, the ratio of the caudate artery origin of the right hepatic arterial system to the left hepatic arterial system was 2.6:1. However, HCCs in the CP were fewer than those in the SP and the PC in the present study. If our cohort had included more tumors in the CP, the number of caudate arteries derived from the right hepatic arterial system might have increased.

The origins of the tumor-feeding caudate arteries may differ among the three subsegment locations of HCC [8, 9, 12]. In the present study, HCCs located in the SP were fed from the caudate arteries derived from the right and left hepatic arterial systems (the ratio of right to left = 3:2). In addition, the extrahepatic vessels infrequently feed HCCs in the SP, in particular those located at the liver surface. HCCs in the PC were also fed by the caudate arteries derived from the right and left hepatic arterial systems, with a lower frequency arising from the left hepatic arterial supply (the ratio of right to left = 3:1). Almost all HCCs in the CP were dominantly fed by the caudate artery derived from the right hepatic arterial system, mainly arising from the anterior or posterior segmental artery of the right hepatic artery. This tendency may be helpful to identify the tumor-feeding caudate artery according to the tumor location. Yoon et al. [9] also reported a similar tendency, although the incidences of blood supply to HCCs in the PC from the left hepatic arterial system were low compared with those in our series. We selected patients with HCCs in the caudate lobe that had not previously been treated. However, 62% of patients had previously undergone TACE for other HCCs before detection of HCCs in the

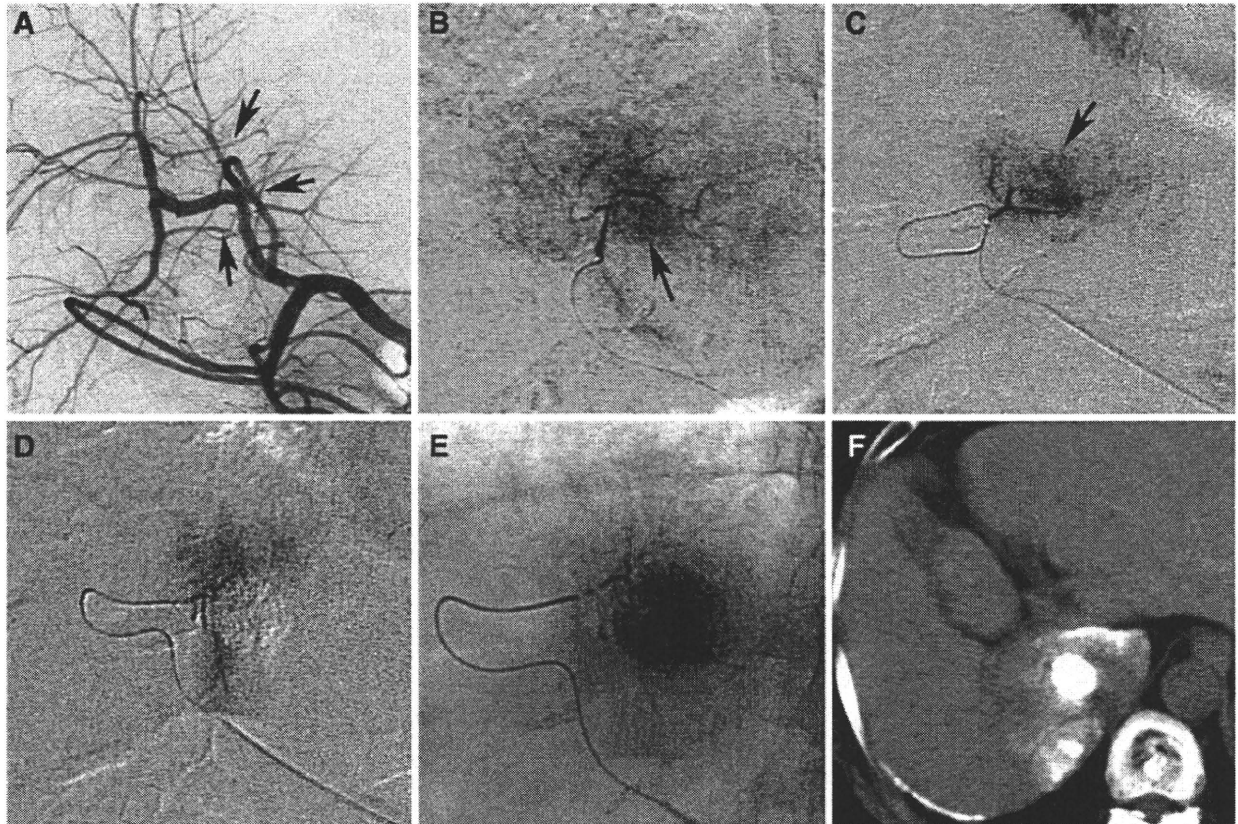


Fig. 6 A 75-year-old woman with HCC in the PC. **A** Celiac arteriogram showed three caudate arteries (arrows). **B** The caudate artery derived from the distal portion of the right hepatic artery was selected and arteriogram showed a tumor stain (arrow). TACE was performed at this point. **C** The caudate artery deriving from the posterior segmental artery of the right hepatic artery was selected, and the arteriogram also showed a tumor stain (arrow). TACE was

performed. **D** The caudate artery deriving from the anterior segmental artery of the right hepatic artery was selected, and TACE was performed. **E** Spot radiograph obtained during TACE showed dense iodized oil accumulation in the tumor. **F** CT obtained 1 week after TACE showed dense iodized oil accumulation in HCC and the caudate lobe

Table 4 Feeding arteries of 14 HCCs in the CP

No. of feeders	No. of tumors (%)	Site	Origin	Tumor
1	9 (64.3)	R	R ₁	1
			A	3
			P	3
			M	1
			Ph	1
2	4 (28.6)	R × 2	R ₁ , R ₂	1
			R ₂ , A	1
			A × 2	1
			P × 2	1
3	1 (7.1)	R × 3	R ₂ , P × 2	1

Mean tumor diameter 21.8 ± 12.9 mm [range 12–49]

caudate lobe. Previous TACE through the neighboring branches of the caudate lobe might have changed the vascular territories of the caudate arteries.

There are several limitations in the present study. First, we did not evaluate the caudate arteries that were identified on arteriogram, but that did not supply the tumor, because we could not definitely confirm whether these vessels exactly supplied the caudate lobe on angiographic findings alone. Therefore, our study did not analyze the origins of all of the caudate arteries, and this might strongly influence the number and origin of the caudate arteries detected. Three-dimensional CT during hepatic arteriography, using a multidetector-row CT, may provide sufficient information about the caudate arteries, including those that do not supply the tumor. Second, the number of tumor-feeding caudate arteries might easily change according to the tumor size. In large tumors, small caudate branches may become hypertrophied enough to be depicted on arteriogram, and parasitization of the extrahepatic collateral vessels may also become apparent. Finally, there was a possibility of missing small tumor-feeding caudate branches, although iodized oil was accumulated in all tumors throughout the

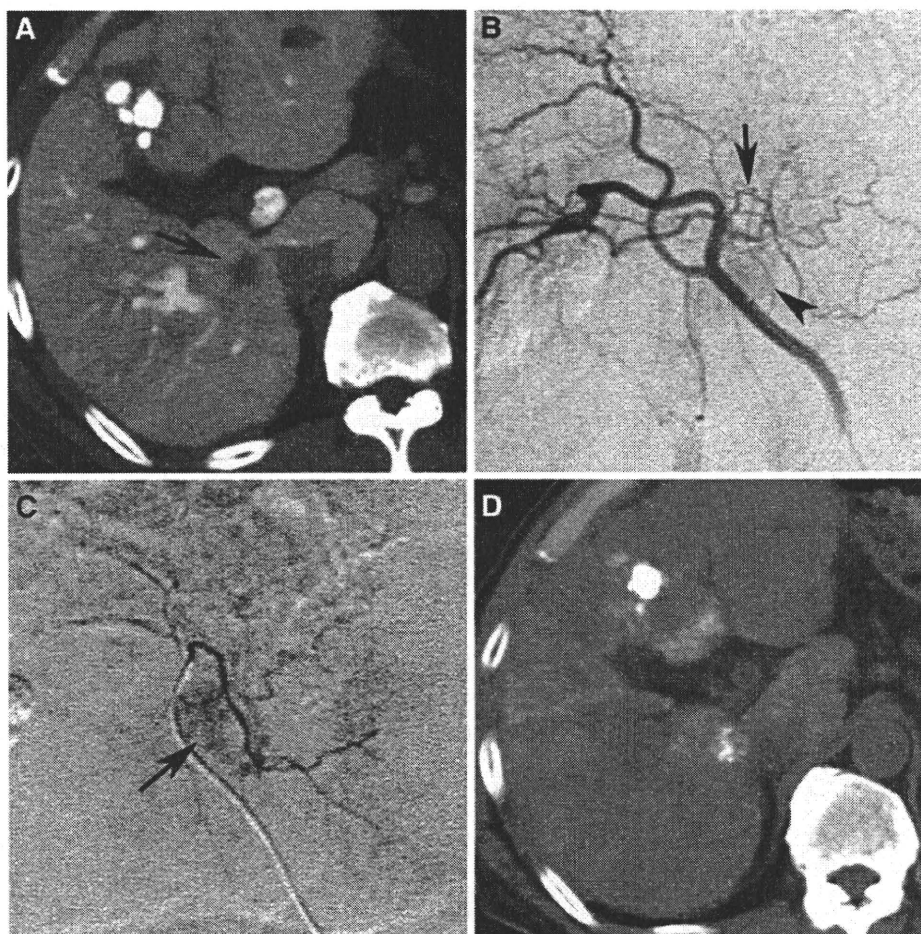


Fig. 7 A 64 year-old man with HCC in the CP. **A** CT during arterial portography showed a tumor in the CP (*arrow*). The tumor with iodized oil accumulation that had previously been embolized was also seen in segment 4. **B** Arteriogram of the right hepatic artery showed that the caudate artery derived from the posterior segmental artery of

the right hepatic artery (*arrow*). The *arrowhead* shows a tumor stain. **C** The caudate artery was selected and embolized. The *arrow* showed a tumor stain. **D** CT obtained 1 week after TACE showed iodized oil accumulation in HCC in the CP

entire tumor portion after TACE, including those after six additional TACE sessions. Because multiple caudate arteries are frequently connected not only with each other but also with neighboring branches, iodized oil might also flow into the tumor through unidentified small caudate branches by way of these communications [16, 17].

In conclusion, the tumor-feeding caudate artery most frequently arose from the right hepatic artery, followed with almost equal frequency by the left hepatic artery, the anterior segmental artery of the right hepatic artery, and the posterior segmental artery of the right hepatic artery. HCCs located in the SP were fed by the caudate artery derived from both hepatic arteries (the ratio of right to left = 3:2); HCCs in the PC were also fed by both hepatic arteries (the ratio of right to left = 3:1); and HCCs in the CP were dominantly fed by the caudate artery derived from the right

hepatic artery. We consider that recognition of this tendency may be helpful to identify the tumor-feeding caudate artery on angiogram.

Conflict of Interest None.

References

1. Takayasu K, Muramatsu Y, Shima Y et al (1986) Clinical and radiologic features of hepatocellular carcinoma originating in the caudate lobe. *Cancer* 58:1557–1562
2. Tanaka S, Shimada M, Shirabe K et al (2005) Surgical outcome of patients with hepatocellular carcinoma originating in the caudate lobe. *Am J Surg* 190:451–455
3. Shimada M, Matsumata T, Maeda T et al (1994) Characteristics of hepatocellular carcinoma originating in the caudate lobe. *Hepatology* 19:911–915

4. Shibata T, Maetani Y, Ametani F et al (2002) Efficacy of non-surgical treatments for hepatocellular carcinoma in the caudate lobe. *Cardiovasc Intervent Radiol* 25:186–192
5. Seror O, Haddad D, N'Konkhou G et al (2005) Radiofrequency ablation for the treatment of liver tumors in the caudate lobe. *J Vasc Interv Radiol* 16:981–990
6. Yamakado K, Nakatsuka A, Akeboshi M et al (2005) Percutaneous radiofrequency ablation for the treatment of liver neoplasms in the caudate lobe left of the vena cava: electrode placement through the left lobe of the liver under CT-fluoroscopic guidance. *Cardiovasc Intervent Radiol* 28:638–640
7. Miyayama S, Matsui O, Kameyama T et al (1990) Angiographic anatomy of arterial branches to the caudate lobe of the liver: with special reference to its effect on transarterial embolization of hepatocellular carcinoma. *Jpn J Clin Radiol* 35:353–359 (in Japanese)
8. Terayama N, Miyayama S, Tatsu H et al (1998) Subsegmental transcatheter arterial embolization for hepatocellular carcinoma in the caudate lobe. *J Vasc Interv Radiol* 9:501–508
9. Yoon CJ, Chung JW, Cho BH et al (2008) Hepatocellular carcinoma in the caudate lobe of the liver: angiographic analysis of tumor-feeding arteries according to subsegmental location. *J Vasc Interv Radiol* 19:1543–1550
10. Mizumoto R, Suzuki H (1988) Surgical anatomy of the hepatic hilum with special reference to the caudate lobe. *World J Surg* 12:2–10
11. Suzuki H (1982) Correlation and anomalies of the vascular stricture in Glisson's area around the hepatic hilum, from the standpoint of hepatobiliary surgery. *Arch Jpn Chir* 51:713–731 (in Japanese)
12. Miyayama S, Yamashiro M, Yoshie Y et al (2010) Hepatocellular carcinoma in the caudate lobe of the liver: variations of its feeding branches on arteriography. *Jpn J Radiol* 28:555–562
13. Kumon M (1985) Anatomy of the caudate lobe with special reference to portal vein and bile duct. *Acta Hepatol Jpn* 26:1193–1199 (in Japanese)
14. Matsui O, Kadoya M, Yoshikawa J et al (1993) Small hepatocellular carcinoma: treatment with subsegmental transcatheter arterial embolization. *Radiology* 188:79–83
15. Miyayama S, Matsui O, Yamashiro M et al (2007) Ultrasensitive transcatheter arterial chemoembolization with a 2-F tip microcatheter for small hepatocellular carcinomas: relationship between local tumor recurrence and visualization of the portal vein with iodized oil. *J Vasc Interv Radiol* 18:365–376
16. Miyayama S, Yamashiro M, Okuda M et al (2010) Main bile duct stricture occurring after transcatheter arterial chemoembolization for hepatocellular carcinoma. *Cardiovasc Intervent Radiol* 33:1168–1179
17. Miyayama S, Matsui O, Taki K et al (2005) Arterial blood supply to the posterior aspect of segment IV of the liver from the caudate branch: demonstration at CT after iodized oil injection. *Radiology* 237:1110–1114

Hepatocellular carcinoma in the caudate lobe of the liver: variations of its feeding branches on arteriography

Shiro Miyayama · Masashi Yamashiro · Yuichi Yoshie
Yoshiko Nakashima · Hiroshi Ikeno · Nobuaki Orito
Miki Yoshida · Osamu Matsui

Received: March 26, 2010 / Accepted: May 27, 2010
© Japan Radiological Society 2010

Abstract There are usually multiple caudate arteries arising from the right, left, and middle hepatic arteries, and they are frequently connected to each other. Therefore, hepatocellular carcinoma (HCC) in the caudate lobe is frequently fed by multiple branches arising from different origins. HCC located in the Spiegel lobe is usually fed by the caudate arteries derived from the right and/or left hepatic artery. HCC in the paracaval portion is mainly fed by the caudate artery derived from the right hepatic artery; with low frequency, it is fed by the caudate artery derived from the left hepatic artery. HCC in the caudate process is usually fed by the caudate artery derived from the right hepatic artery. Because of the complexity and overlap of vascular territories, the tumor-feeding branch of a recurrent HCC lesion in the caudate lobe frequently changes on follow-up arteriograms. In addition, several extrahepatic collateral vessels supply the recurrent tumor. To perform effective transcatheter arterial chemoembolization (TACE) for HCC in the caudate lobe, radiologists should have sufficient knowledge of vascular anatomy supplying HCC in the caudate lobe.

Key words Hepatocellular carcinoma · Caudate lobe · Vascular anatomy · Chemoembolization

S. Miyayama (✉) · M. Yamashiro · Y. Yoshie · Y. Nakashima · H. Ikeno, N. Orito · M. Yoshida
Department of Diagnostic Radiology, Fukuiken Saiseikai Hospital, 7-1 Funabashi, Wadanaka-cho, Fukui 918-8503, Japan
Tel. +81-776-23-1111; Fax +81-776-28-8519
e-mail: s-miyayama@fukui.saiseikai.or.jp

O. Matsui
Department of Radiology, Kanazawa University Graduate School of Medical Science, Kanazawa, Japan

Introduction

The caudate lobe is centrally located in the liver, between the right and left lobes. Because of this anatomical location, hepatocellular carcinoma (HCC) arising in the caudate lobe is difficult to treat. Surgical resection of the caudate lobe has a high mortality rate, in addition to a high recurrence rate of the tumor.^{1,2} Percutaneous ablation therapy (e.g., radiofrequency ablation) is a useful alternative treatment,^{3,4} but the procedure might be technically difficult because of the deep tumor location and adjacent large vessels. Therefore, transcatheter arterial chemoembolization (TACE) plays an important role in the treatment of HCC in the caudate lobe.^{5,6}

Because there are usually multiple caudate arteries arising from the right, left, and middle hepatic arteries, HCC in the caudate lobe is frequently fed by multiple branches arising from different origins.^{5,9} In addition, the feeding branches become more complex when the tumor recurs after TACE. These factors might make it more difficult to control HCC in the caudate lobe by TACE. To perform effective TACE for HCC in the caudate lobe, radiologists should have sufficient knowledge of vascular anatomy supplying HCC in the caudate lobe.

Subsegments of the caudate lobe

The caudate lobe is divided into three subsegments according to portal vein ramification: Spiegel lobe, paracaval portion, caudate process. The Spiegel lobe is the protuberant hepatic portion to the left of the intrahepatic vena cava.¹⁰ The paracaval portion is in front of the intrahepatic vena cava and is surrounded by the right

and middle hepatic veins.^{10,11} The caudate process is a tongue-like projection between the vena cava and adjacent portal vein.¹⁰ Theoretically, there are multiple caudate arteries supplying these three subsegments.

Caudate artery anatomy

A cadaver dissection study by Mizumoto and Suzuki⁷ reported that the caudate arteries arose from the posterior segmental artery of the right hepatic artery and left hepatic artery in 32.1%, from the posterior segmental artery of the right hepatic artery and middle hepatic artery in 26.4%, and from the three arteries in 20.8%. However, in a previous angiographic observation, the incidences of the caudate artery derived from the left hepatic artery and the posterior segmental artery of the right hepatic artery were low. Because the left hepatic lobe has limited depth, identification of the caudate artery is difficult even on stereo-arteriograms.⁹ In addition, the caudate artery derived from the posterior segmental artery is frequently difficult to recognize because it mimics the posterior segmental artery of the right hepatic artery.⁹

With advances in digital subtraction angiography systems and catheter technology, two or more caudate arteries arising from the right hepatic, middle hepatic, and/or left hepatic artery can be demonstrated in almost all cases. In the right hepatic artery, the caudate artery arises between the proximal portion of the right hepatic artery and the main trunk of the anterior or posterior segmental artery of the right hepatic artery (Figs. 1–7). On the left side, the caudate artery usually arises between the proximal portion and umbilical portion of the left hepatic artery (Figs. 3, 8). The caudate artery also arises from the proximal portion of the middle hepatic artery or medial segmental artery (Fig. 9). It infrequently arises

with the cystic artery as a common trunk (Fig. 10). Additionally, it infrequently arises from the proper hepatic (Fig. 11), common hepatic, or extrahepatic artery (Fig. 12).

Among the caudate arteries derived from the right hepatic artery, the paracaval branch runs upwardly (Fig. 4), and the Spiegel lobe branch runs to the left (Figs. 1–5, 11). These branches frequently arise as a common trunk (Figs. 4, 13). Selective arteriography of the Spiegel lobe branch shows a typical hepatogram indicating the contour of the Spiegel lobe (Figs. 1, 9, 11, 13). The caudate process branch usually mimics the posterior segmental artery of the right hepatic artery (Fig. 13). Among the caudate arteries derived from the left hepatic artery, the Spiegel lobe branch usually mimics the lateral segmental artery (Fig. 3), and the paracaval branch mimics the medial segmental artery (Figs. 9, 13).

The caudate arteries are frequently connected to each other as well as to the medial segmental artery (Fig. 7).^{12–14}

Hepatocellular carcinoma

HCC in the Spiegel lobe

HCC located in the Spiegel lobe is usually fed by the caudate arteries derived from the right and/or left hepatic artery.^{5,6} Almost all feeding branches mainly arise from the proximal portion of the right and left hepatic artery (Figs. 1–3). In addition, the caudate artery arising from the proximal portion of the middle hepatic or medial segmental artery supplies tumors in the Spiegel lobe (Fig. 9). Because the Spiegel lobe protrudes from the liver, a large tumor is frequently found to be fed by extrahepatic collateral vessels at the initial discovery.

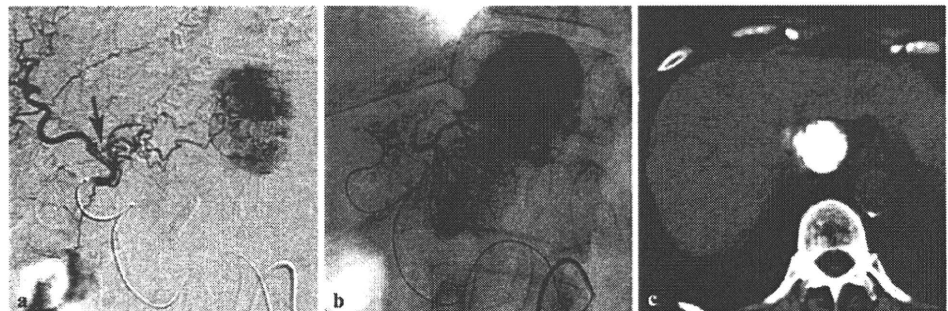


Fig. 1. Hepatocellular carcinoma (HCC) in the Spiegel lobe. **a** Arteriogram of the right hepatic artery shows a tumor stain in the Spiegel lobe supplied by the caudate artery derived from the right hepatic artery (arrow). **b** The caudate artery was selected, and

transcatheter arterial chemoembolization (TACE) was performed. The contour of the Spiegel lobe is clearly seen. **c** Computer tomography (CT) 1 week after TACE shows dense iodized oil accumulation in the tumor

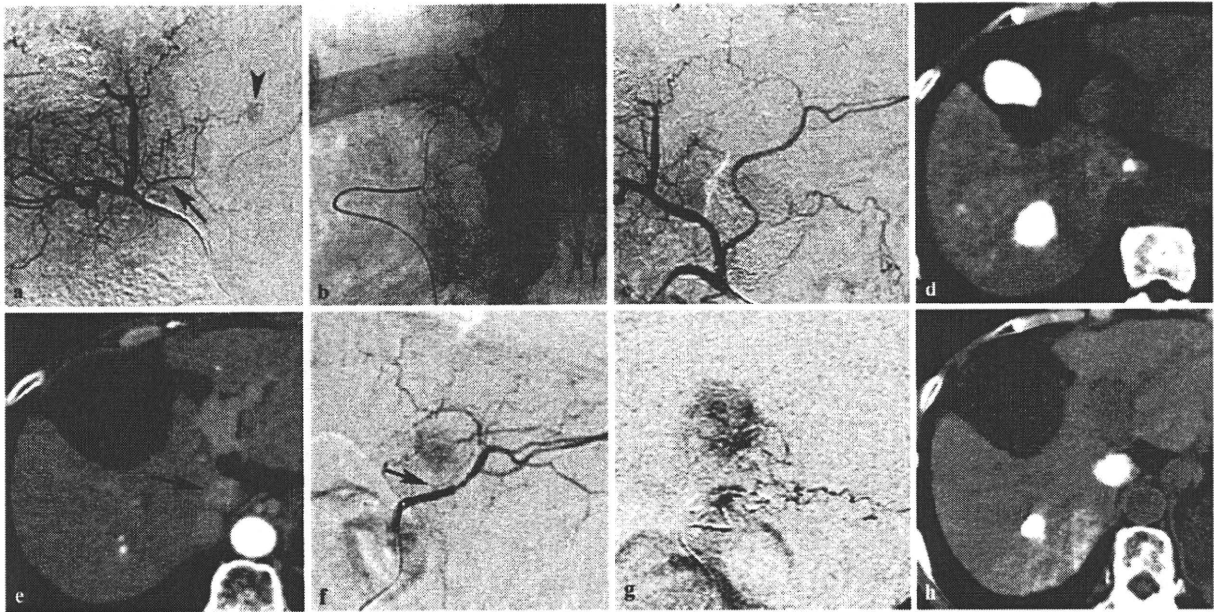


Fig. 2. HCC in the Spiegel lobe. **a** Arteriogram of the right hepatic artery obtained after TACE of the anterosuperior subsegmental artery of the right hepatic artery shows a tumor stain (*arrowhead*) supplied by the caudate artery derived from the anterior segmental artery of the right hepatic artery (*arrow*). **b** The caudate artery was selected, and TACE was performed. The contour of the Spiegel lobe was clearly seen. *Arrow* points to the tumor. **c** Proper hepatic arteriogram obtained immediately after TACE shows no residual

tumor stain. **d** CT 1 week after TACE shows dense iodized oil accumulation in both tumors. **e** Arterial phase CT 3 years after TACE shows a recurrent tumor in the Spiegel lobe (*arrow*). **f** Follow-up arteriogram shows a tumor stain supplied by the caudate artery derived from the left hepatic artery (*arrow*) that was not seen in **c**. **g** The branch was selected, and TACE was performed. **h** CT 1 week after additional TACE shows dense iodized oil accumulation in the tumor

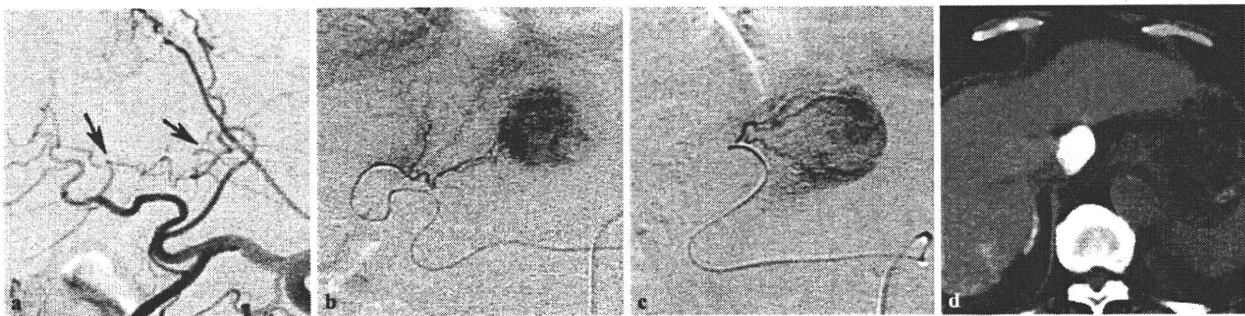


Fig. 3. HCC in the Spiegel lobe. **a** Celiac arteriogram shows two caudate arteries derived from the right and left hepatic artery, respectively (*arrows*). **b** First, the caudate artery derived from the right hepatic artery was selected, and TACE was performed. **c** Second, the caudate artery derived from the left hepatic artery was

selected, and TACE was performed. **d** CT 1 week after TACE shows dense iodized oil accumulation in the tumor. Iodized oil was also accumulated in the right adrenal gland because the right inferior phrenic artery was subsequently embolized to treat another tumor (not shown)

HCC in the paracaval portion

When HCC is in the paracaval portion, it is mainly fed by the caudate artery derived from the right hepatic artery.^{5,6} Several feeding branches frequently arise between the right hepatic artery and the proximal portion of the anterior or posterior segmental artery of the right hepatic artery (Fig. 6). Another feeding branch also

arises from the left hepatic artery (Fig. 13). The tumor in the paracaval portion is rarely supplied by the caudate artery derived from the left hepatic artery alone (Fig. 8).

HCC in the caudate process

HCC in the caudate process is usually fed by the caudate artery derived from the right hepatic artery (Fig. 4).^{5,6}

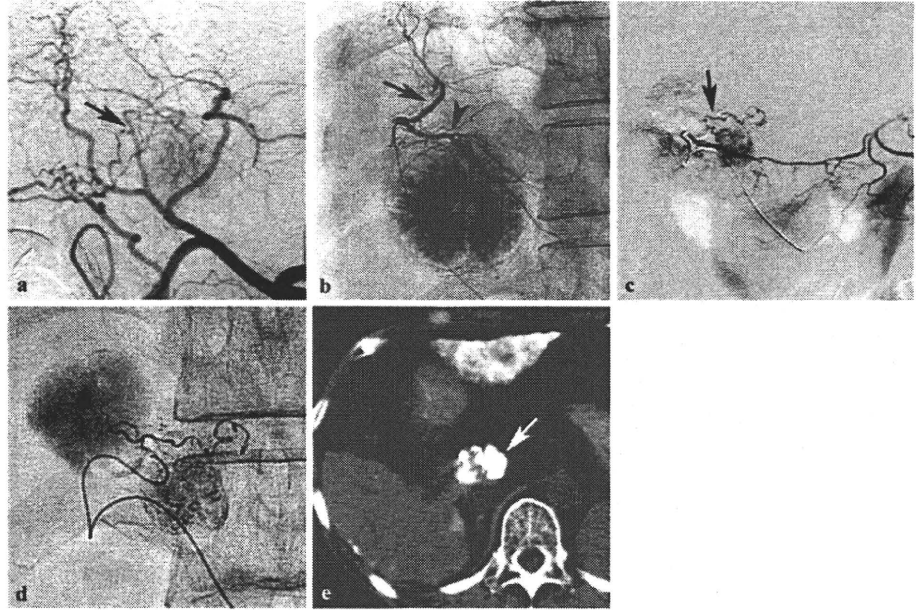


Fig. 4. HCC in the caudate process. **a** Celiac arteriogram shows a tumor stain supplied by the hypertrophied caudate artery derived from the right hepatic artery (*arrow*). **b** Spot radiograph obtained during TACE showed that the Spiegel branch (*arrowhead*) and paracaval branch (*arrow*) arose as a common trunk. **c** Two years later, a new lesion developed near the previous tumor site. Ar-

teriogram of the right gastric artery shows a tumor stain supplied by a small branch (*arrow*). **d** The branch was selected, and TACE was performed. **e** CT 1 week after TACE shows dense iodized oil accumulation in the tumor (*arrow*). Iodized oil was also seen in the left lobe of the liver because the left hepatic artery was subsequently embolized to treat other tumors (not shown)

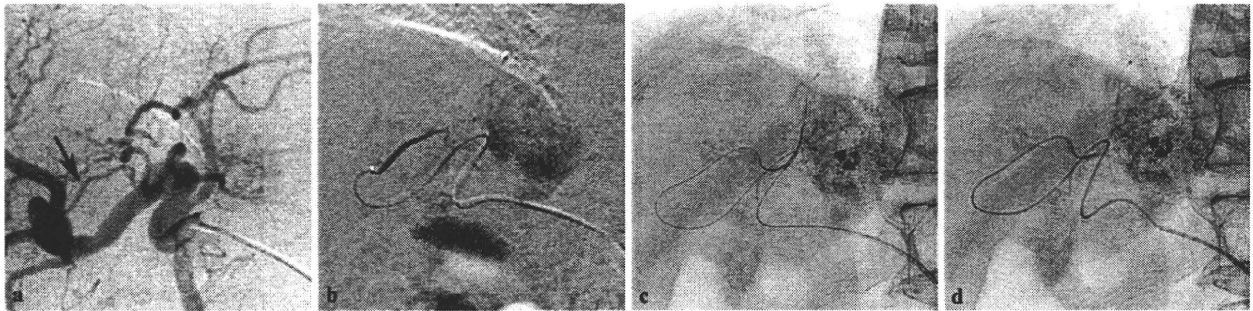


Fig. 5. HCC in the Spiegel lobe. **a** Celiac arteriogram shows a tumor stain supplied by the right hepatic artery (*arrow*). **b** The caudate artery was selected using a shaped microcatheter. The guidewire was advanced into the caudate artery, but the micro-

catheter could not be advanced into it. **c** The shaped microcatheter was withdrawn and exchanged for a thinner flexible microcatheter. **d** The microcatheter was deeply advanced into the caudate artery using an over-the-wire technique, and TACE was completed

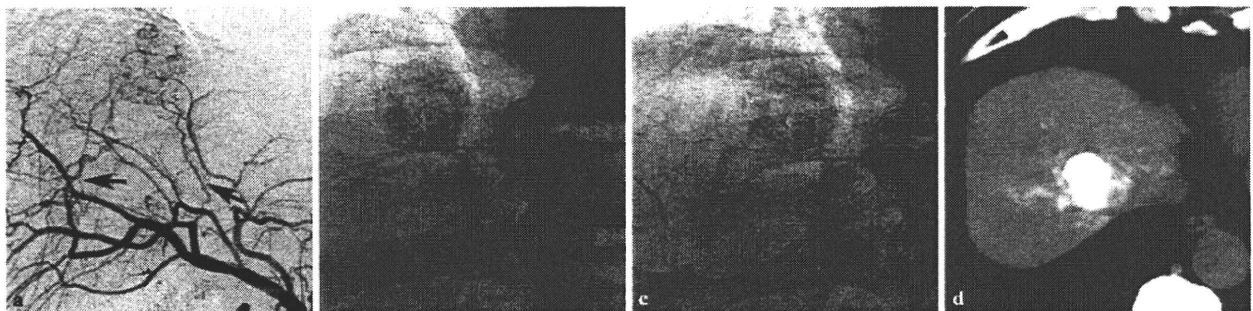


Fig. 6. HCC in the paracaval portion. **a** Common hepatic arteriogram shows a tumor stain supplied by two caudate arteries derived from different sites (*arrows*). **b** First, the caudate artery derived from the anterior segmental artery of the right hepatic artery was

selected and TACE was performed. **c** Second, the caudate artery derived from another anterior segmental artery of the right hepatic artery was selected, and TACE was performed. **d** CT 1 week after TACE shows dense iodized oil accumulation in the tumor

Fig. 7. HCC in the Spiegel lobe. **a** Celiac arteriogram shows two caudate arteries derived from the anterior segmental artery of the right hepatic artery (*arrows*). **b** First, one of the caudate arteries was selected, and TACE was performed. **c** Second, another caudate artery was selected, and TACE was started. **d** Arteriogram obtained during TACE shows the left hepatic artery through the anastomosis (*arrow*). **e** Then, the microcatheter was advanced distally to the anastomosed branch, and TACE was completed. **f** CT 1 week after TACE shows dense iodized oil accumulation in the tumor

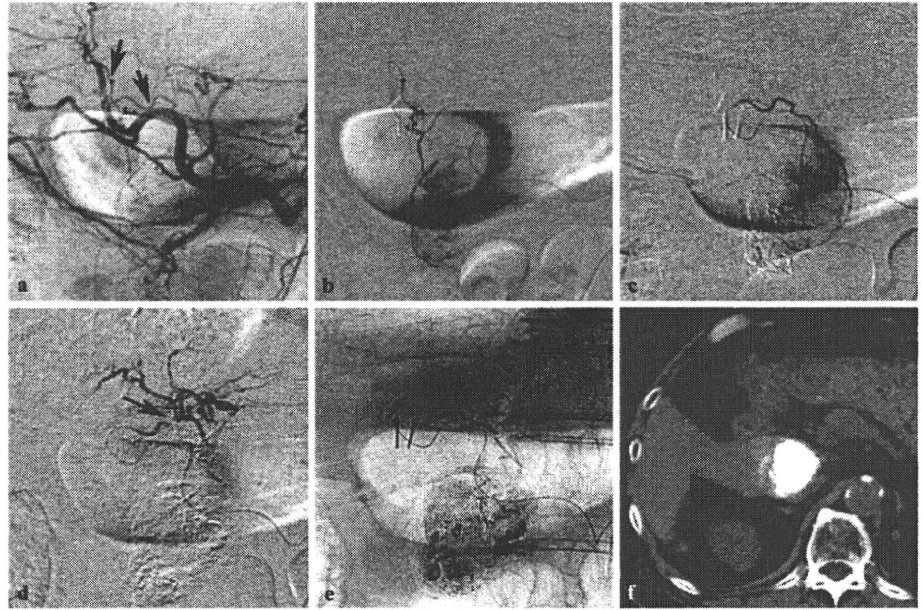


Fig. 8. HCC in the paracaval portion. **a** Arteriogram of the left hepatic artery shows a tumor stain supplied by the caudate artery derived near the umbilical portion of the left hepatic artery (*arrow*). **b** The vessel was selected, and TACE was performed. **c** CT 1 week after TACE shows dense iodized oil accumulation in the tumor

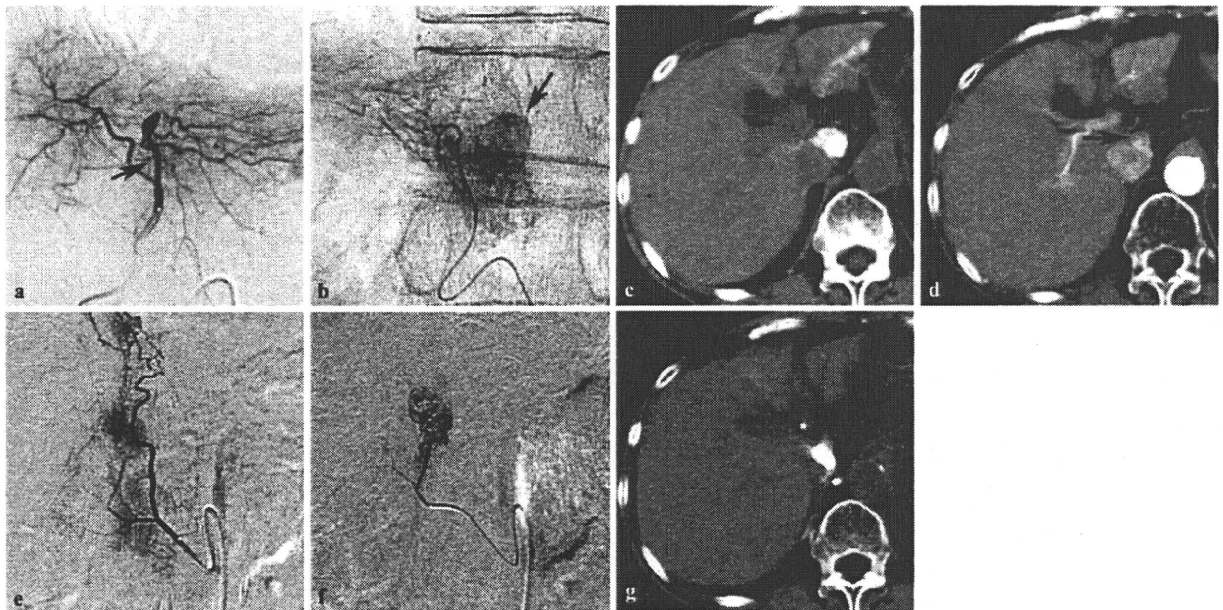
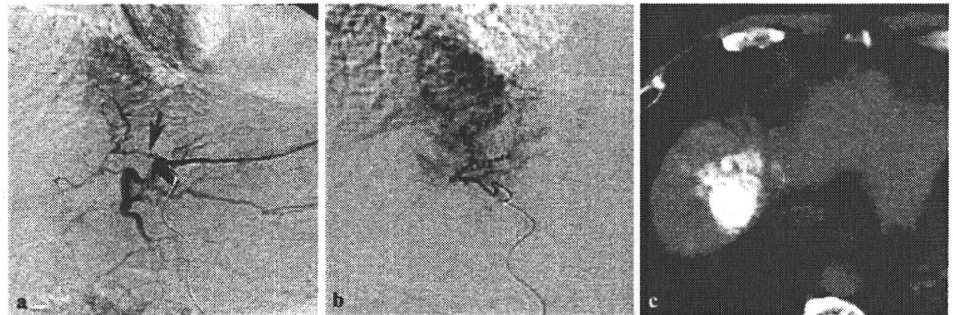


Fig. 9. HCC in the Spiegel lobe. **a** Arteriogram of the left hepatic artery shows the caudate artery derived from the medial segmental artery (*arrow*). **b** The vessel was selected, and TACE was performed. **c** The contour of the Spiegel lobe was seen. *Arrow* points to the tumor. **d** CT 1 week after TACE shows dense iodized oil accumulation in the tumor. **e** However, CT 13 months after TACE

shows a recurrent tumor (*arrow*). **e** On additional angiography, the previously embolized caudate artery was occluded (not shown). The tumor was supplied by the right inferior phrenic artery alone. **f** The tumor-feeding branch was selected, and TACE was performed. **g** CT 1 week after TACE shows dense iodized oil accumulation in the tumor

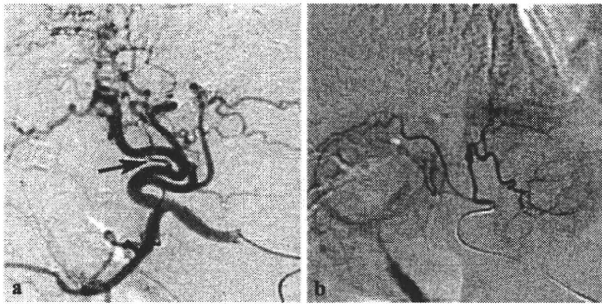


Fig. 10. Caudate artery derived from the cystic artery. **a** Common hepatic arteriogram shows that the cystic artery derived from the proximal portion of the right hepatic artery (*arrow*). **b** Selective arteriogram shows that the caudate artery was derived from the cystic artery

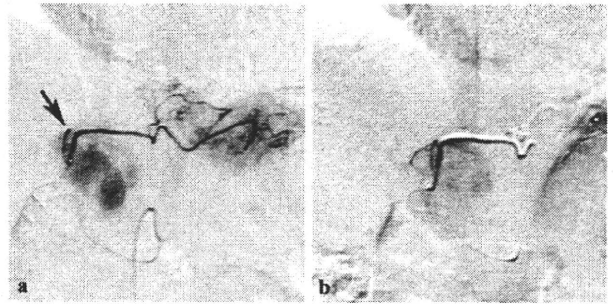


Fig. 12. HCC in the Spiegel lobe. **a** Arteriogram of the accessory left gastric artery shows a tumor stain supplied by a small branch (*arrow*). **b** The branch could not be directly selected; therefore, TACE was performed after embolization of the accessory left gastric artery using metallic coils and *n*-butyl-cyanoacrylate

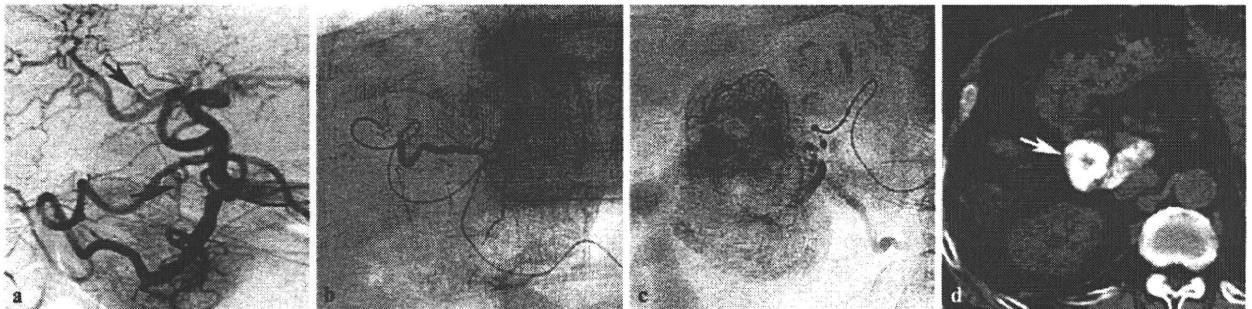


Fig. 11. HCC in the caudate process. **a** Common hepatic arteriogram shows two caudate arteries (*arrow*). **b** First, the Spiegel lobe branch derived from the right hepatic artery was selected, and TACE was performed. The contour of the Spiegel lobe is clearly

seen. **c** Second, the caudate process branch derived from the proper hepatic artery was selected, and TACE was performed. This vessel was a main feeder of the tumor. **d** CT 1 week after TACE shows dense iodized oil accumulation in the tumor (*arrow*)

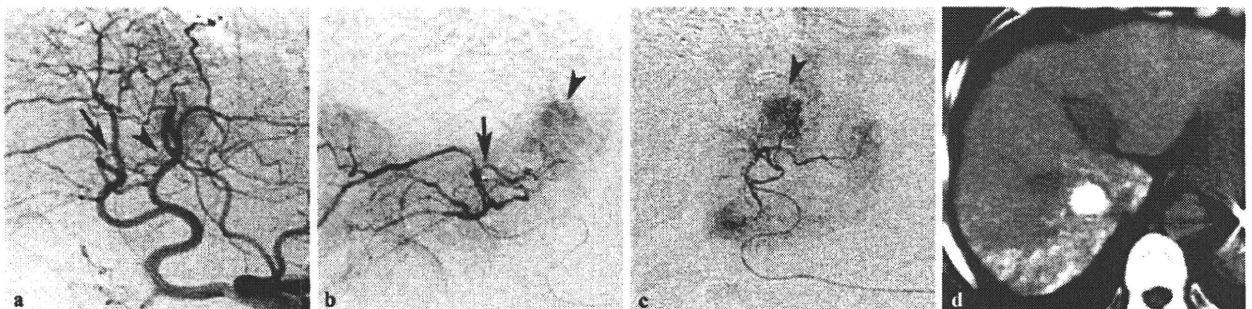


Fig. 13. HCC in the paracaval portion. **a** Celiac arteriogram shows two caudate arteries derived from the left hepatic artery (*arrowhead*) and the posterior segmental artery of the right hepatic artery (*arrow*). **b** Arteriogram of the posterior segmental artery of the right hepatic

artery shows a tumor stain (*arrowhead*). *Arrow* indicates the caudate artery. **c** Arteriogram of the caudate artery derived from the left hepatic artery also shows the tumor stain (*arrowhead*). **d** CT 1 week after TACE shows dense iodized oil accumulation in the tumor

Fig. 14. Recurrent HCC in the Spiegel lobe. **a** Arteriogram of the left gastric artery shows a tumor (arrowhead) supplied by a small branch (arrow). **b** The branch was selected, and TACE was performed. **c** CT 1 week after TACE shows dense iodized oil accumulation in the tumor

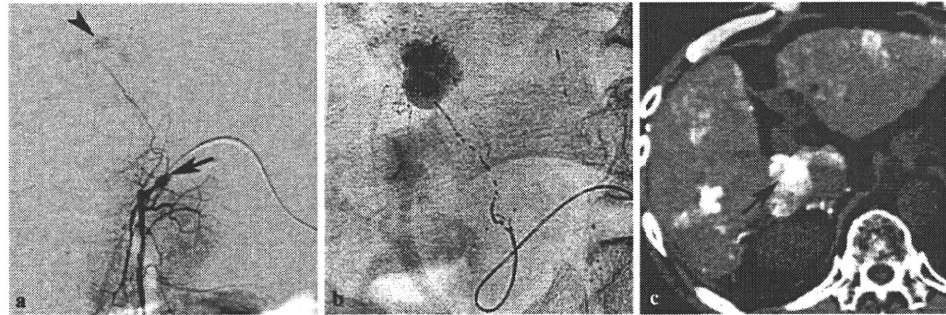
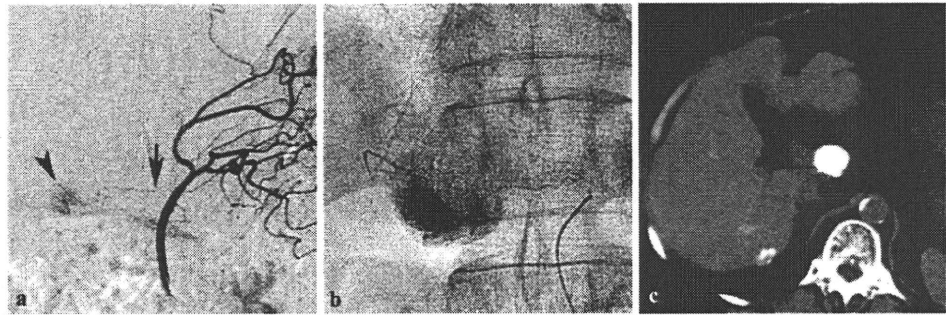


Fig. 15. Recurrent HCC in the caudate process. **a** Arteriogram of the posterosuperior pancreaticoduodenal artery shows a small tumor stain (arrowhead) supplied by the 3 o'clock and 9 o'clock

arteries (arrow). **b** The vessel was selected, and TACE was performed. **c** CT 1 week after TACE shows dense iodized oil accumulation in the tumor (arrow)

The caudate artery derived from the proper hepatic artery also supplies tumors in the caudate process (Fig. 11).

Changes in tumor-feeding branches of recurrent tumors

Because of the presence of multiple caudate arteries and the overlap of these vascular territories, the tumor-feeding branch of a recurrent tumor in the caudate lobe frequently changes on follow-up arteriograms.⁶ Another caudate artery arising from a different origin replaces the tumor-feeding branch; in particular, a small feeding branch becomes sufficiently hypertrophied to be detected on angiography (Fig. 2).

Extrahepatic arteries frequently supply the recurrent tumor in the caudate lobe, particularly the tumor in the Spiegel lobe. The right inferior phrenic (Fig. 9), right or left gastric (Figs. 4, 14), dorsal pancreatic, right adrenal, and right renal capsular arteries are possible collateral vessels for recurrent tumors in the Spiegel lobe. The 3 o'clock and 9 o'clock arteries are also possible collateral vessels for recurrent tumors in the caudate process (Fig. 15). In addition, recurrent HCC in the paracaval portion is supplied by the right inferior phrenic artery.

Catheterization technique in the caudate artery

Owing to proximal branching of the caudate artery, non-selective TACE is not effective for HCC in the caudate lobe.^{8,9} Because the caudate artery usually has a small caliber, a microcatheter with a tip less than 2F facilitates selective catheterization. As the caudate artery frequently arises at an acute angle, shaping the microcatheter by steam-heating is useful for selective catheterization. When the tip of the microcatheter faces the orifice of the caudate artery, a guidewire is inserted into the caudate artery, and the microcatheter is then advanced into the branch. An over-the-wire technique to exchange the shaped microcatheter for a flexible one is also useful if the shaped microcatheter cannot be advanced into the caudate artery (Fig. 5). For arterial blockage distal to the caudate artery, use of a microballoon catheter has been reported.¹⁵ In a small branch derived from extrahepatic collateral pathways, embolization using a metallic coil and/or *n*-butyl-cyanoacrylate at the distal portion of the small feeding branch is also useful when it cannot be directly selected (Fig. 12).

Multiple caudate arteries frequently anastomose to each other to form an arcade.^{12–14} When the embolic materials are injected from one of the caudate arteries,

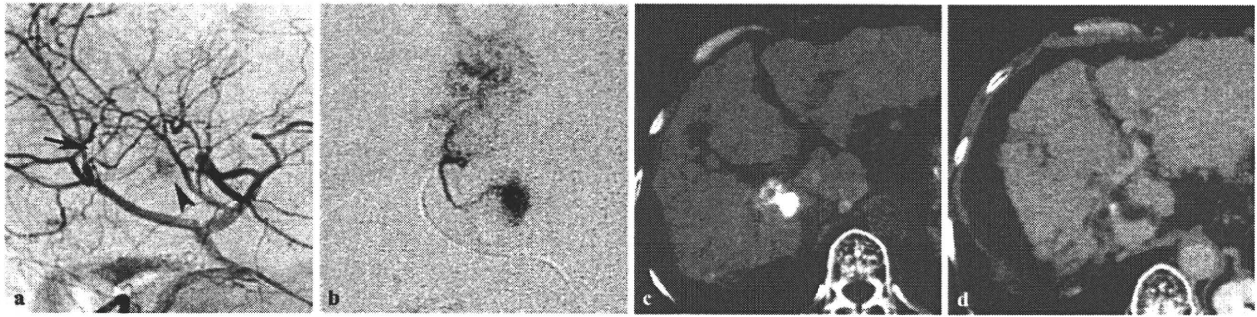


Fig. 16. Bile duct dilatation after TACE of the caudate artery. **a** Common hepatic arteriogram shows a small tumor stain (arrowhead) supplied by the caudate artery derived from the anterior segmental artery of the right hepatic artery (arrow). **b** The caudate artery was selected, and TACE was performed.

c CT 1 week after TACE shows dense iodized oil accumulation in the tumor. **d** CT 6 years after TACE shows that the tumor was well controlled. However, the bile duct was dilated in the right lobe of the liver, and the right lobe of the liver was atrophied

collateral blood flow through the other caudate arteries reverses the blood flow in the embolized artery and pushes back the embolic materials.⁵⁹ If possible, the microcatheter should be advanced distal to the anastomosis branch to avoid inadvertent widespread embolization (Fig. 7). Small branches supplying the main bile duct usually arise from the caudate artery¹²; therefore, bile duct stricture may occur after TACE of the caudate artery (Fig. 16).¹⁴ This is a rare but serious complication of TACE through the caudate artery.

Conclusion

The caudate artery usually arises from the proximal portion of the hepatic artery. The vascular supply to HCC in the caudate lobe is complex because of the presence of multiple caudate arteries and their overlapped vascular territories. In addition, several extrahepatic collateral vessels feed recurrent tumors in the caudate lobe. Identification of the tumor-feeding caudate artery and selective catheterization is essential to perform effective TACE.

References

1. Tanaka S, Shimada M, Shirabe K, Maehara S, Tsujita E, Taketomi A, et al. Surgical outcome of patients with hepatocellular carcinoma originating in the caudate lobe. *Am J Surg* 2005;190:451–5.
2. Shimada M, Matsumata T, Maeda T, Yanaga K, Taketomi A, Sugimachi K. Characteristics of hepatocellular carcinoma originating in the caudate lobe. *Hepatology* 1994;19:911–5.
3. Shibata T, Maetani Y, Ametani F, Kubo T, Itoh K, Konishi J. Efficacy of nonsurgical treatments for hepatocellular carcinoma in the caudate lobe. *Cardiovasc Intervent Radiol* 2002;25:186–92.
4. Yamakado K, Nakatsuka A, Akeboshi M, Takaki H, Takeda K. Percutaneous radiofrequency ablation for the treatment of liver neoplasms in the caudate lobe left of the vena cava: electrode placement through the left lobe of the liver under CT-fluoroscopic guidance. *Cardiovasc Intervent Radiol* 2005;28:638–40.
5. Terayama N, Miyayama S, Tatsu H, Yamamoto T, Toya D, Tanaka N, et al. Subsegmental transcatheter arterial embolization for hepatocellular carcinoma in the caudate lobe. *J Vasc Interv Radiol* 1998;9:501–8.
6. Yoon CJ, Chung JW, Cho BH, Jae HJ, Kang SG, Kim HC, et al. Hepatocellular carcinoma in the caudate lobe of the liver: angiographic analysis of tumor-feeding arteries according to subsegmental location. *J Vasc Interv Radiol* 2008;19:1543–50.
7. Mizumoto R, Suzuki H. Surgical anatomy of the hepatic hilum with special reference to the caudate lobe. *World J Surg* 1998;12:2–10.
8. Takayasu K, Muramatsu Y, Shima Y, Goto H, Moriyama N, Yamada T, et al. Clinical and radiologic features of hepatocellular carcinoma originating in the caudate lobe. *Cancer* 1986;58:1557–62.
9. Miyayama S, Matsui O, Kameyama T, Hirose J, Konishi H, Choto S, et al. Angiographic anatomy of arterial branches to the caudate lobe of the liver; with special reference to its effect on transarterial embolization for hepatocellular carcinoma. *Jpn J Clin Radiol* 1990;35:353–9 (in Japanese).
10. Kumon M. Anatomy of the caudate lobe with special reference to portal vein and bile duct. *Acta Hepatol Jpn* 1985;26:1193–9 (in Japanese).
11. Matsui O, Takashima T, Kadoya M, Hirose J, Kameyama T, Choto S, et al. CT anatomy of para-caval portion of the caudate lobe of the liver. *Nippon Igaku Hoshasen Gakkai Zasshi* 1988;48:841–6 (in Japanese).
12. Stapleton GN, Hickman R, Terblanche J. Blood supply of the right and left hepatic ducts. *Br J Surg* 1998;85:202–7.
13. Miyayama S, Matsui O, Taki K, Minami T, Ryu Y, Ito C, et al. Arterial blood supply to the posterior aspect of segment IV of the liver from the caudate branch: demonstration at CT after iodized oil injection. *Radiology* 2005;237:1110–4.
14. Miyayama S, Yamashiro M, Okuda M, Yoshie Y, Nakashima Y, Ikeno H, et al. Main bile duct stricture occurring after transcatheter chemoembolization for hepatocellular carcinoma. *Cardiovasc Intervent Radiol* 2010 Jan 8. [Epub ahead of print].
15. Ishimaru H, Ishimaru K, Mitarai K, Koshiishi T, Matsuoka Y, Egawa A, et al. Application of coaxial micro-balloon catheter (Attendant) for treatment of hepatocellular carcinoma. *Jpn J Intervent Radiol* 2007;22:72–5 (in Japanese).

Complex comprised of dextran magnetite and conjugated cisplatin exhibiting selective hyperthermic and controlled-release potential

Akinaga Sonoda¹
 Norihisa Nitta¹
 Ayumi Nitta-Seko¹
 Shinich Ohta¹
 Shigeyuki Takamatsu²
 Yoshio Ikehata³
 Isamu Nagano³
 Jun-ichiro Jo⁴
 Yasuhiko Tabata⁴
 Masashi Takahashi¹
 Osamu Matsui³
 Kiyoshi Murata¹

¹Department of Radiology, Shiga University of Medical Science, Setatsukinowa-cho, Otsu, Shiga, 520-2192, Japan; ²Department of Radiology, Graduate School of Medical Science, Kanazawa University, Takaramachi 13-1, Kanazawa Ishikawa, 920-8641, Japan; ³Department of Natural Science and Technology, Graduate School of Engineering, Kanazawa University, Kakuma-machi, Kanazawa, Ishikawa 920-1192, Japan; ⁴Department of Biomaterials, Institute for Frontier Medical Sciences, Kyoto University, Shogoin kawara-machi 53, Sakyo-ku 606-8507, Kyoto, Japan

Correspondence: Akinaga Sonoda
 Department of Radiology, Shiga University of Medical Science, Setatsukinowa-cho, Otsu, Shiga 520-2192, Japan
 Tel +81-77-548-2285
 Fax +81-77-544-0986
 Email akinaga@belle.shinga-med.ac.jp

Abstract: We developed a dextran-magnetite conjugated cisplatin (DM-Cis) complex for use in thermal ablation and as a chemotherapeutic drug. To produce DM-Cis we reacted Cis with 1 mL DM (56 mg/mL iron). The temperature rise of DM-Cis was measured *in vitro* and *in vivo* under a portable induction-heating (IH) device. Platinum desorption from DM-Cis over 24 hours was measured in bovine serum. In *in vivo* accumulation and magnet and exothermic experiments we used four rat groups. In group 1 we delivered DM-Cis intraperitoneally (ip) and placed magnets subcutaneously (sc). In group 2 we injected saline (ip) and placed magnets (sc). In group 3 we injected DM-Cis (ip) and placed a sc incision (sham). The control (group 4) received an ip injection of saline. Rectus abdominis muscle tissue was stained with hematoxylin-eosin and iron-stained tissue areas (μm^2) were calculated. The maximum platinum concentration in DM-Cis was approximately 105.6 $\mu\text{g/mL}$. Over 24 hours, 33.48% of platinum from DM-Cis was released. There was a significant difference ($P < 0.05$) in the iron-stained area between group 1 and the other groups. The temperature in muscle tissue registered a maximum of 56°C after about 4 min. DM-Cis may represent a magnetically-accumulated anticancer drug with hyperthermic effects.

Keywords: magnetic nanoparticle-conjugated anticancer agents, DM, portable induction heating device, carboxyl group, rat

Introduction

The purpose of this study was to develop a DM-Cis complex and to examine the possibility of using DM-Cis for hyperthermic treatment and chemotherapy.

Magnetic nanoparticles have been used to diagnose tumors in the liver and spleen by magnetic resonance imaging (MRI).¹ The *in vivo* accumulation of these particles in specific areas has been studied and the feasibility of hyperthermic treatment with magnetic particles has been investigated.²⁻¹⁰ As magnetic nanoparticles convert energy absorbed from an alternating magnetic field into heat, they may be useful for the delivery of hyperthermic therapy. Murata et al¹¹ reported that anticancer agents delivered intraductally via the nipple may facilitate the administration of neoadjuvant therapy in patients with early breast cancer. We hypothesized that the availability of magnetic nanoparticle-conjugated anticancer agents may make it possible to treat various breast cancers by their intraductal administration and that this treatment would elicit hyperthermic effects.

DM is used widely as a liver-specific contrast medium (Resovist®; Bayer Health Care Japan, Osaka, Japan) and its safety has been established.^{1,8} DM consists of carboxy-dextran, which covers the core and the iron-oxide particles of the core. Therefore, a carboxyl group originating from dextran is present on the particle surface.

The possibility of conjugating DM with the carboxyl group of gelatin and Cis was raised and gelatin-conjugated Cis was found to release Cis slowly, thereby potentially maximizing its anti-tumor effects.^{12,13} (Figure 1).

Methods

Preparation of DM-Cis

A 1:1 ratio was defined as 1 mL Cis (1.43 mg/mL Cis) (Nippon Kayaku Co., Tokyo, Japan) to 1 mL DM (56 mg/mL iron) (Meito, Aichi, Japan). We reacted various amounts of Cis with 1 mL DM. Initially we titrated Cis slowly into DM and followed this procedure with 7-day incubation at 37°C. In subsequent experiments we dialyzed the solution in 10 L of ultrapure double-distilled water (UDDW), exchanging the water 10 times in 7 days; we employed cellulose dialysis tubing (MWCO14000; Viskase Co. Inc., IL, USA) and removed residual unconjugated Cis. The platinum concentration of DM-Cis was measured on an AA-6800 atomic absorption spectrometer (Shimadzu, Kyoto, Japan). When DM was reacted with Cis at a 1:1 ratio, we determined the size of the DM-Cis complex based on dynamic light scattering (DLS; light wave length 514 nm, sample temperature 25°C; Autosizer 4700, Malvern Instruments, Worcestershire, UK).

Exothermic experiment under a magnetic field

A portable IH device (alternating current (AC), 142 KHz magnetic field, single-phase, AC 200 V, electric current 440

Amp, power consumption 3.5 kW) was the magnetic field generator.⁷ After reacting 2.5 mL Cis with 2.5 mL DM, we introduced a polyurethane tube containing 5 mL DM-Cis into the 20-cm diameter IH coil, set the IH device at 142 KHz, and measured the temperature for 10 minutes by inserting a thermometer (FL-2000; Anritsu Meter, Tokyo, Japan) into the tube.

Desorption of platinum from DM-Cis in bovine serum

DM-Cis (3 mL) in cellulose dialysis tubing was immersed in bovine serum (9 mL) and shaken reciprocally (72 strokes/min) at 37°C. At 30 min and 1, 3, 6, 12, and 24 hours we withdrew 0.5-mL bovine serum samples and immediately replaced them with the same volume of fresh bovine serum. The platinum concentration in the samples was then measured on an AA-6800 atomic absorption spectrometer (Shimadzu, Kyoto, Japan).

In vivo accumulation and magnet and exothermic experiments

All experimental protocols were approved by our animal experimentation committee and all experiments were conducted in accord with the Animal Care Guidelines of Shiga University of Medical Science.

Production of the magnet-bearing rat model

Wistar rats (SLC, Tokyo, Japan) were housed for more than one week in solid-floor cages in a dedicated pathogen-free

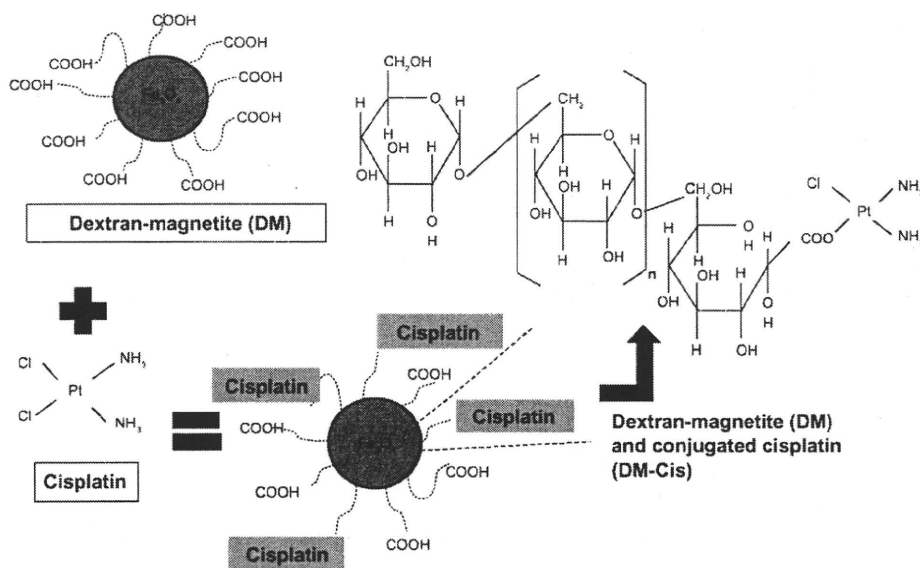


Figure 1 Illustration of a complex comprised of DM and conjugated Cis. A carboxyl group originating from dextran exists partially on the particle surface. The conjugation of DM with the carboxyl group of Cis may result in a slow release of Cis, thereby potentially maximizing its anti-tumor effect.